

Total (elastic and inelastic) scattering cross sections for several positron-molecule systems at 10–5000 eV: H_2 , H_2O , NH_3 , CH_4 , N_2 , CO , C_2H_2 , O_2 , SiH_4 , CO_2 , N_2O , and CF_4

K. L. Baluja* and Ashok Jain

Physics Department, Florida A&M University, Tallahassee, Florida 32307

and Supercomputer Computations Research Institute, Florida State University, Tallahassee, Florida 32306

(Received 22 August 1991)

We report calculations on the total (elastic plus inelastic) positron-scattering cross sections from several diatomic and polyatomic molecules (H_2 , H_2O , NH_3 , CH_4 , N_2 , CO , C_2H_2 , O_2 , SiH_4 , CO_2 , N_2O , and CF_4) where experimental data are available. The impact energy (E) range is 10–5000 eV. A local spherical complex optical potential (SCOP) is calculated for each positron-molecule system from the target charge density $[\rho(r)]$, which in turn is determined from the corresponding molecular wave function at the Hartree-Fock level. The real part of the SCOP is composed of the repulsive static and attractive positron-correlation-polarization potential of Jain [Phys. Rev. A **39**, 2437 (1990)]. The imaginary component of the SCOP, the so-called absorption potential, is derived semiempirically as a function of $\rho(r)$, E , and the mean excitation energy. The resulting complex optical potential is treated exactly in a variable-phase approach to yield complex phase shift and the total-cross-section quantities. In this intermediate- and high-energy region, the small contribution due to the nonspherical nature of the target is neglected. In addition, we fit the total-cross-section values to a simple analytic formula. For molecules possessing a permanent dipole or quadrupole moment, the present results are reliable only roughly above 50 eV.

PACS number(s): 34.80.−i, 34.90.+q, 61.80.Fe

I. INTRODUCTION

The total cross sections (σ_t) (including elastic plus energetically possible all inelastic channels) for positron-molecule systems have recently been measured from low (~ 1 eV) to keV energy region in several laboratories. Table I gives a list of references [1–20], both experimental and theoretical, on the σ_t data for several molecules studied so far. It is clear from Table I that there is hardly any theoretical work above the positronium (Ps) formation energy (E_{Ps}) except the calculations on H_2O , NH_3 , CH_4 , and SiH_4 molecules by one of the authors [18–20]. Several review articles have discussed experimental determination of σ_t for the positron-molecule systems in general (see Refs. [21–26]). A large variety of molecules (H_2 , CO , N_2 , O_2 , CO_2 , N_2O , H_2O , NH_3 , C_2H_2 , CH_4 , SiH_4 , CF_4 , CCl_4 , C_2H_4 , SF_6 , C_2H_6 , C_3H_6 , C_4H_8 , C_4H_{10} , C_6H_6) have been investigated in the laboratory to measure σ_t as a function of impact energy. Recently, Stein and Kaupila [26], Szmytkowski [27], and Sueoka [16] have summarized the σ_t data on the positron-molecule collisions.

At intermediate and high energies ($E \geq 10$ eV), the opening up of several rearrangement (Ps formation, dissociation, etc.), excitation, and ionization channels makes an *ab initio* calculation almost impossible. It is thus quite obvious that most of the calculations carried out so far on the positron-molecule systems have been restricted to low energies (below 10 eV) only. A general discussion on the theory of positron-molecule collisions has recently been given by Armour [28]. The intermediate- and high-energy positron impact calculations on the total cross sections for H_2O , NH_3 , CH_4 , and SiH_4 molecules by Jain [18–20]

employed a simple approach based on the spherical-complex-optical-potential (SCOP) method [29]. The SCOP approach has recently been employed for high-energy electron scattering from a large variety of linear and nonlinear molecules [30]. This paper is an extension of our previous electron work [30]. The discussion on the validity of the SCOP model in general is given in our earlier references [18–20,29].

The basic philosophy of the present method is based on the assumption that the nonspherical nature (providing torque to the molecule for rotational excitation) of the molecular system does not play a significant role in shaping up the total cross section of the high-energy positron-molecule collisions. The collision time is too short and rotational excitation cross sections are insignificant relative to elastic, ionization, etc. processes. In addition, the contribution from the vibrational excitation process is also assumed to be negligible. Below 50 eV, the present results may not be reliable for molecules possessing a permanent dipole or quadrupole moment.

In the next two sections, we provide theoretical details and numerical procedure. The results are discussed in Sec. IV. The concluding remarks are made in the final section, V. We use atomic units in this paper until otherwise specified.

II. THEORY

We first assume that the fixed-nuclei approximation [31] is valid in this energy region and the interaction of the positron-molecule system can be represented by a local complex optical potential, namely,

$$V_{\text{opt}}(\mathbf{r}) = V_R(\mathbf{r}) + iV_{\text{abs}}(\mathbf{r}), \quad (1)$$

where the real part is a sum of repulsive and attractive terms

$$V_R(\mathbf{r}) = V_{\text{st}}(\mathbf{r}) + V_{\text{pol}}(\mathbf{r}). \quad (2)$$

The repulsive static potential $V_{\text{st}}(\mathbf{r})$ is calculated from the unperturbed target wave function Ψ_0 at the Hartree-Fock level (for full details see Ref. [30]). The attractive $V_{\text{pol}}(\mathbf{r})$ represents approximately the short-range correlation and long-range polarization effects. Due to the non-spherical nature of a molecule, the optical potential [Eq. (1)] is not isotropic. A general expression for $V_{\text{opt}}(\mathbf{r})$ for any target can be written in terms of the following multipole expansion around the center of mass of the molecule [32],

$$V_{\text{opt}}^{p\mu}(\mathbf{r}) = \sum_{l,h} v_{lh}(r) X_{lh}^{(p\mu)}(\hat{\mathbf{r}}), \quad (3)$$

where $(p\mu)$ denotes the ground-state symmetry of molecule and the symmetry adapted X functions are defined in terms of real spherical harmonics $S_{lm}^{\pm}(\hat{\mathbf{r}})$ (see Ref. [32]),

$$X_{lh}^{(p\mu)}(\hat{\mathbf{r}}) = \sum_{m=0}^{+l} b_{lhm}^{(p\mu)} S_{lm}^q(\hat{\mathbf{r}}). \quad (4)$$

For closed-shell systems, the $(p\mu)$ is the totally symmetric 1A_1 (nonlinear molecules) or ${}^1\Sigma_g^+$ (linear molecules) irreducible representation. The values of allowed l , h , m , etc. depend on a particular point-group symmetry of the molecule. The anisotropic terms, $l=1,2,\dots$, in expansion (3), provide torque to excite rotational levels in the molecule. As mentioned earlier, our main assumption in this work is that such higher-order terms are weak and can be neglected in the present intermediate- and high-energy region. However, it is essential to average the optical potential [Eq. (3)] over all molecular orientations and use the averaged (spherical) potential $[(1/4\pi) \int V_{\text{opt}}^{p\mu}(\mathbf{r}) d\hat{\mathbf{r}}]$ derived from Eq. (1) to be $v_{0l}(r)/\sqrt{4\pi}$.

First we determine the target charge density $\rho(\mathbf{r})$ of a given molecule,

$$\rho(\mathbf{r}) = \int |\Psi_0|^2 d\mathbf{r}_1 d\mathbf{r}_2 \cdots d\mathbf{r}_Z = 2 \sum_{\alpha} |\phi_{\alpha}(\mathbf{r})|^2, \quad (5)$$

where Z is the number of electrons in the target, ϕ_i is the i th molecular orbital, and a factor of 2 appears due to spin integration and the α sum being over each doubly occupied orbital. All the three potential terms (V_{st} , V_{pol} , and V_{abs}) are a function of $\rho(\mathbf{r})$. For example,

TABLE I. Summary of total cross sections (σ_t) available in the literature for positron scattering with various molecules. Note that the low-energy (below E_{ps}) calculations are excluded from the following reference list. The last eight molecules are not investigated in the present work.

Molecule	Experiment data (energy range in eV)	Theory (energy range in eV)
H ₂	(21.5–600) ^a ; (1–500) ^b ; (8–400) ^c ; (2.15–20.84) ^d	
CH ₄	(19–600) ^a ; (2.15–19.86) ^d ; (5–400) ^e ; (1–400) ^f	(20–500) ^g
NH ₃	(1–400) ⁱ	(1–400) ^j
H ₂ O	(1–400) ^k	(1–400) ^j
N ₂	(16.5–600) ^a ; (0.5–750) ^b ; (2.28–22.21) ^d	
	(1–400) ^l ; (1–3000) ^{m,n}	
CO	(1–400) ^l ; (1–500) ^o	
C ₂ H ₂	(1–400) ^p	
O ₂	(1–500) ^h ; (14–600) ^a ; (2.03–22.48) ^d	
SiH ₄	(1–400) ^f	(10–500) ^q
CO ₂	(14.5–600) ^a ; (0.5–60) ^b ; (1.76–22.48) ^d	
	(30–500) ^e ; (1–500) ^l	
N ₂ O	(1–500) ^r	
CF ₄	(1–400) ^s	
C ₂ H ₄	(5–400) ^e ; (1–400) ^f	
C ₂ H ₆	(5–400) ^e	
C ₃ H ₆	(5–400) ^e	
C ₄ H ₈	(5–400) ^e	
C ₄ H ₁₀	(5–400) ^e	
C ₆ H ₆	(1–400) ^t	
SF ₆	(5–500) ^h	
CCl ₄	(1–400) ^s	

^aReference [1].

^bReference [2].

^cReference [3].

^dReference [4].

^eReference [5].

^fReference [6].

^gReference [18].

^hReference [7].

ⁱReference [8].

^jReference [19].

^kReference [9].

^lReference [10].

^mReference [11].

ⁿReference [12].

^oReference [13].

^pReference [14].

^qReference [20].

^rReference [15].

^sReference [16].

^tReference [17].

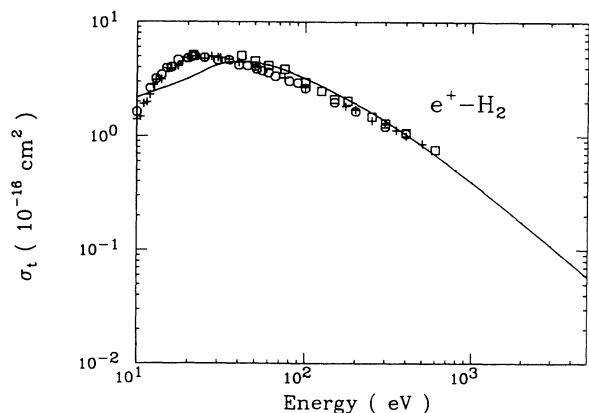


FIG. 1. Total cross sections for the positron- H_2 case. Present calculations are shown by solid curve. The experimental data are from Refs. [2] (+), [3] (o), and [1] (□).

$$V_{\text{st}}(\mathbf{r}) = \int \rho(\mathbf{r}_1) |\mathbf{r} - \mathbf{r}_1|^{-1} d\mathbf{r}_1 - \sum_{i=1}^M Z_i |\mathbf{r} - \mathbf{R}_i|^{-1}. \quad (6)$$

The V_{pol} is calculated in the positron-correlation-polarization (PCOP) approximation recently proposed by one of the authors [33–35]. The PCOP potential is based on the correlation energy $\epsilon_{\text{cor}}(r_s)$ (where r_s is the density parameter) of a single positron in a homogeneous electron gas. In the outside region, the ϵ_{cor} is joined smoothly with the well-known correct asymptotic form of the polarization potential (for example, $\alpha_0/2r^4$; α_0 is the target polarizability in a.u.) where they cross each other for the first time. In a way, this procedure is quite similar to the electron-correlation-polarization (ECOP) potential of O'Connell and Lane [36] suggested for electron-atom collisions. Later, the ECOP approach was modified and employed for molecular systems [37,38]. This PCOP potential, like the ECOP one, is parameter-free and a function of the target charge density. Physically, the two models (ECOP and PCOP) are quite different from each other [33–35]. In our previous positron- CH_4 (SiH_4) calculations [19,20], we employed ECOP approximation to include target polarization effects. In our recent low-

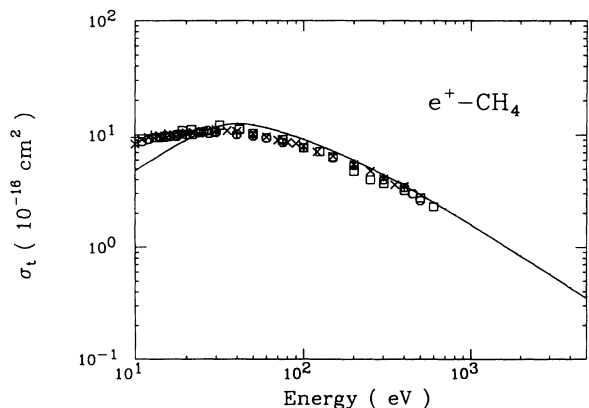


FIG. 2. Total cross sections for the positron- CH_4 case. Present results are shown by solid curve. Experimental data: Ref. [5], +; Ref. [7], o; Ref. [6], x; Ref. [1], □.

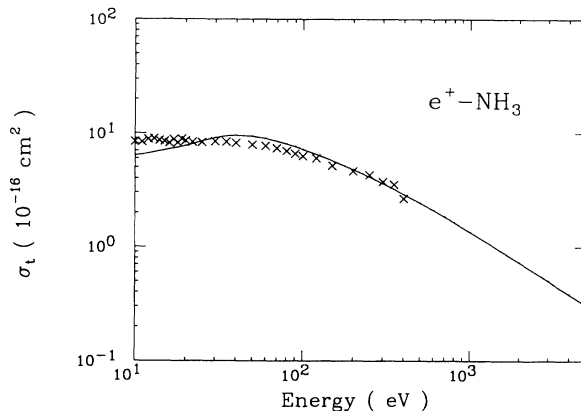


FIG. 3. Same as in Fig. 2 but for NH_3 case. The experimental points (x) are from Ref. [8].

energy positron-molecule calculations [39–41], we have shown that the PCOP model is more realistic than the corresponding ECOP approximation used as such for positron scattering.

Thus an accurate evaluation of $\rho(\mathbf{r})$ is important in our SCOP model. We employed various single-center expansion programs to determine the charge density and various potentials for linear [42] and nonlinear [43] molecules. The ALAM code of Morrison [42] was modified to include more than two nuclei; thus for the present C_2H_2 molecule, the modified version of ALAM (to be denoted here as MALAM [44]) generates single-center quantities of any planar molecule. For linear targets in this study, we obtained molecular wave functions from published tables [45,46], while for nonlinear cases we employed the MOLMON computer code [47]. In the present high-energy region, an exact representation of polarization and correlation effects is not very important.

The imaginary part of the optical potential, $V_{\text{abs}}(\mathbf{r})$, is the absorption potential which represents approximately the combined effect of all the inelastic channels. An *ab initio* calculation of absorption potential is still an open problem. Here we employ a local absorption potential derived semiempirically from the electron absorption potential (V_{abs}^-) of Truhlar and co-workers [48]. The V_{abs}^- is

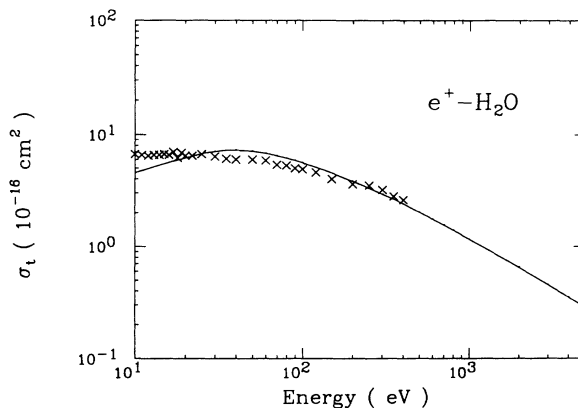


FIG. 4. Same as in Fig. 3 but for H_2O case. The experimental points (x) are from Ref. [9].

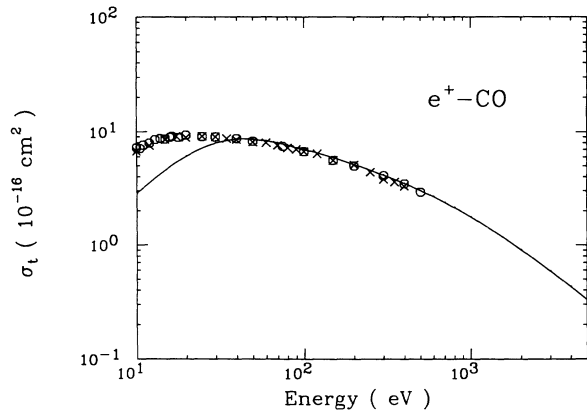


FIG. 5. Same as in Fig. 3 but for the CO molecule. The experimental data are from Refs. [10] (\times) and [13] (\circ).

a function of molecular charge density, incident electron energy, and the mean excitation energy Δ of the target (see Refs. [48]). The absorption (σ_{abs}) and the σ_t cross sections depend significantly on the choice of the value of Δ ; however, we have taken $\Delta = E_{\text{Ps}}$. The final form of the present positron absorption interaction (V_{abs}^+) is determined empirically once for all the energies for different targets. In brief, the V_{abs}^+ is derived from the corresponding V_{abs}^- as follows:

$$V_{\text{abs}}^+(r) = \frac{c}{\sqrt{kr}} V_{\text{abs}}^-(r). \quad (7)$$

Some justification of using a form like that in Eq. (7) will be discussed below. The value of c in (7) is kept the same at all energies, but varies between one and two in different targets (see below).

After generating the full averaged optical potential of a given positron-molecule system, we treat it exactly in a partial-wave analysis by solving the following set of first-order coupled differential equations for the real (χ_l) and imaginary ($\bar{\chi}_l$) parts of the complex phase-shift function under the variable-phase-approach (VPA) [49]:

$$\chi_l'(kr) = -\frac{2}{k} [2V_R(r)(A^2 - B^2) + 2V_{\text{abs}}(r)AB], \quad (8)$$

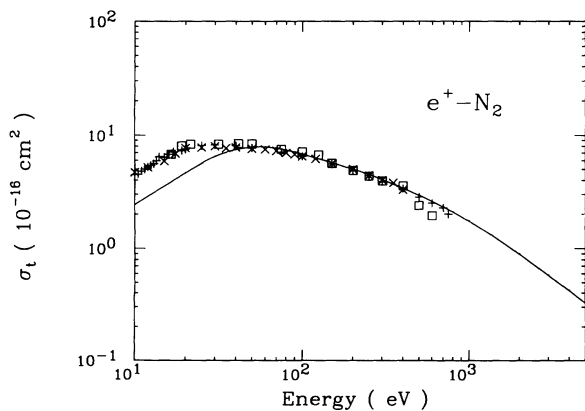


FIG. 6. Same as in Fig. 5 but for the N_2 molecule. The measured points are from Refs. [2] ($+$), [1] (\square), and [10] (\times).

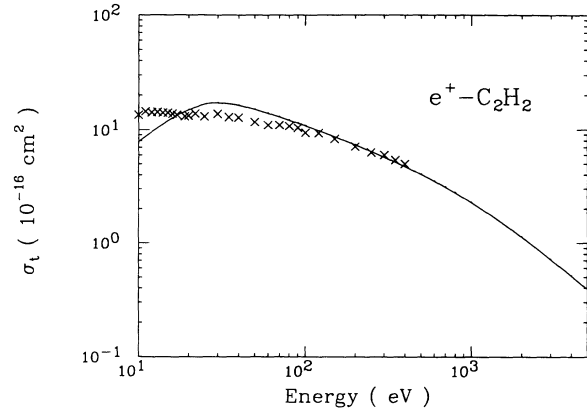


FIG. 7. Same as in Fig. 6 except for the C_2H_2 case. The experimental points (\times) are from Ref. [14].

$$\bar{\chi}_l'(kr) = -\frac{2}{k} [2V_R(r)AB - 2V_{\text{abs}}(r)(A^2 - B^2)], \quad (9)$$

where

$$A = \cosh \bar{\chi}_l(kr) [\cos \chi_l(kr) j_l(kr) - \sin \chi_l(kr) \eta_l(kr)], \quad (10a)$$

$$B = -\sinh \bar{\chi}_l(kr) [\sin \chi_l(kr) j_l(kr) - \cos \chi_l(kr) \eta_l(kr)], \quad (10b)$$

and $j_l(kr)$ and $\eta_l(kr)$ are the usual Riccati-Bessel functions [49]. Equations (8) and (9) are integrated up to a sufficiently large r different for different l and k values. Thus the final S matrix is written as

$$S_l(k) = \exp(-2\bar{\chi}_l) \exp(i2\chi_l). \quad (11)$$

The integrated elastic (σ_{el}), σ_{abs} and σ_t cross sections are described in terms of the S matrix as follows:

$$\sigma_{\text{el}}^l = \frac{\pi}{k^2} (2l+1) |1 - S_l(k)|^2, \quad \sigma_{\text{el}} = \sum_{l=0}^{l_{\text{max}}} \sigma_{\text{el}}^l, \quad (12)$$

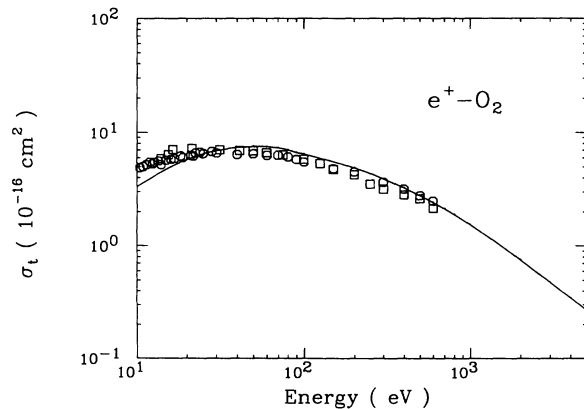


FIG. 8. Positron- O_2 total cross sections. Present results (solid line); experimental data are taken from Refs. [7] (\circ) and [1] (\square).

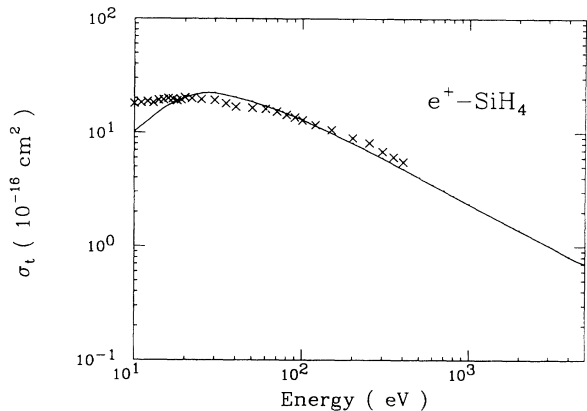


FIG. 9. Positron-SiH₄ total cross sections. Present results, solid line; experimental data (×) are taken from Ref. [6].

$$\sigma_{\text{abs}}^l = \frac{\pi}{k^2} (2l+1) [1 - |S_l(k)|^2], \quad \sigma_{\text{abs}} = \sum_{l=0}^{l_{\text{max}}} \sigma_{\text{abs}}^l, \quad (13)$$

$$\sigma_t^l = \frac{2\pi}{k^2} (2l+1) [1 - \text{Re}S_l(k)], \quad \sigma_t = \sum_{l=0}^{l_{\text{max}}} \sigma_t^l. \quad (14)$$

We note that $\sigma_t = \sigma_{\text{el}} + \sigma_{\text{abs}}$ is the contribution from the spherical term only. In the above analysis the inelasticity or the absorption factor is defined by $|S_l(k)| = \exp(-2\bar{\chi}_l)$.

III. NUMERICAL DETAILS

In order to solve Eqs. (8) and (9), we need a large number of partial waves [l_{max} in Eqs. (12)–(14)] in the present intermediate- and high-energy region. We carried out convergence tests with respect to radial distance and the step size to preserve numerical accuracy. The value of l_{max} varied from 20 to 400 depending upon the impact energy. The V_{abs}^+ is a short-range potential and does not require more than 30 partial waves at the highest energy of the present energy region. In Table II, we have provided the values of E_{Ps} , α_0 , and c [Eq. (7)] parameters for

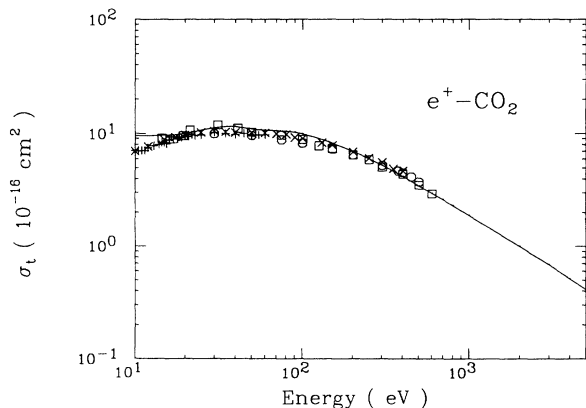


FIG. 10. Positron-CO₂ total cross sections. Present calculations, solid curve; the measured data are from Refs. [1] (□), [13] (○), [10] (×), and [2] (+).

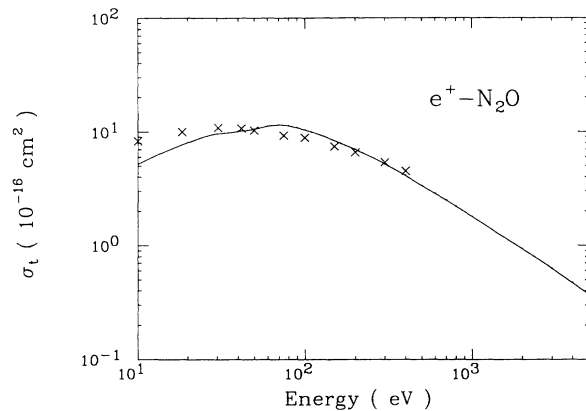


FIG. 11. Positron-N₂O total cross sections. Present results (solid line); experimental points (×) are from Ref. [15].

each molecule studied in this paper.

The justification of choosing $V_{\text{abs}}^+(r)$ in terms of $V_{\text{abs}}^-(r)$ [Eq. (7)] comes from the following argument: The $V_{\text{abs}}^-(r)$ is a function of target charge density, projectile energy, Fermi momentum, mean excitation energy, etc. It is also a well-known fact that evaluation of $V_{\text{abs}}^-(r)$ is a very difficult problem from an *ab initio* point of view. For the present e^+ case, $V_{\text{abs}}^-(r)$ is different from the corresponding e^- case since the $V_{\text{ex}}(r)$ (exchange potential) is zero and the $V_{\text{st}}(r)$ (static potential) is repulsive. In the original derivation of $V_{\text{abs}}^-(r)$ (see Ref. [48]), the imposed conditions that (i) the initially unbound e^- is not allowed to fall into the occupied Fermi sea, and (ii) the lowest-energy state is available to the initially bound e^- , exceeding the Fermi level by the energy gap (Δ), are also valid for the present positron scattering. Also note that a factor of $\frac{1}{2}$ that approximately accounts for the exchange interaction in the original derivation of $V_{\text{abs}}^-(r)$ (see Ref. [48]) is removed in the present calculation of $V_{\text{abs}}^-(r)$ for e^+ in Eq. (7). Thus the choice of $V_{\text{abs}}^+(r)$ in terms of $V_{\text{abs}}^-(r)$ is fully justified [note that actual numerical values of $V_{\text{abs}}^-(r)$ for e^- and e^+ are different]. Also we do not know the actual relationship between $V_{\text{abs}}^+(r)$ and $V_{\text{abs}}^-(r)$, therefore a simple relationship [Eq. (7)] assumed in this

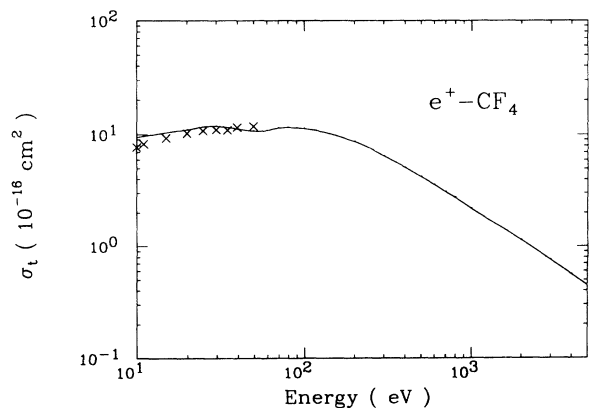


FIG. 12. Positron-CF₄ total cross sections. Present results (solid line); experimental points (×) are from Ref. [16].

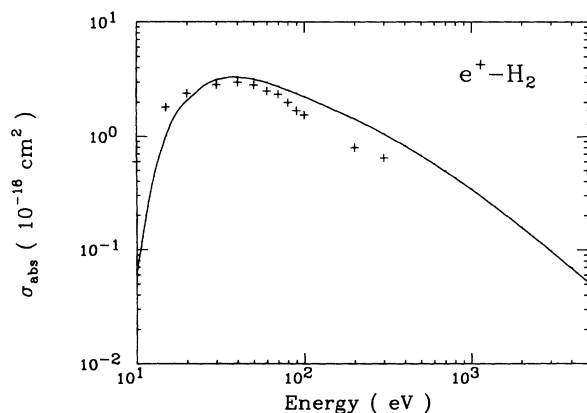


FIG. 13. Absorption cross sections for positron-H₂ collisions in the present theory (solid line). The + points are the measured values (Ref. [51]) of total ionization plus positronium formation cross sections.

work can only be justified by its success in reproducing experimental data for a large number of targets as will be demonstrated below. The presence of the arbitrary factor \sqrt{kr} in Eq. (7) may be justified approximately as follows: at the lower end of the present energy region (10–100 eV), the Ps formation channel has significant effect on the shape and magnitude of the total cross section. Therefore, in an approximate way, the factor \sqrt{kr} may be taking care of the Ps formation channel in an attempt to modify the absorption potential. In addition, we have found that the form [Eq. (7)] gives a good comparison of $V_{\text{abs}}^+(r)$ for rare gases between present results and the calculation of Joachain and Potvlige [50].

IV. RESULTS AND DISCUSSION

For all the above 12 molecules, our σ_t values are shown in Figs. 1–12 along with various experimental results (see Table I). We see a good agreement between our theoretical and experimental data at all energies except below 30 eV for some gases. The maximum in σ_t as observed in experimental data is well reproduced at the appropriate energy. The peaking behavior in σ_t is mainly due to the ionization channel (see following discussion).

Figure 1 shows the e^+ -H₂ σ_t values along with several sets of experimental data. We notice from Fig. 1 that beyond 30 eV, our values are in good accord with the measured cross sections. However, some discrepancies between theory and experiment are observed in the 10–50-eV energy region: our σ_t curve exhibits a peaking structure around 40 eV in contrast to the experimental shape around 20 eV. This difference is not surprising because it is very difficult to mimic the large correlation effects in H₂ in the present simple approach.

In Fig. 2 we have compared our e^+ -CH₄ total cross sections with available experimental data (see Table I). Here the hump in the observed σ_t data around 40 eV is clearly reproduced in our theoretical curve. Our results at and above 20 eV shown in Fig. 2 lie within experimental error bar (not shown). The total cross sections for NH₃ and H₂O are displayed in Figs. 3 and 4, respectively, along with the only measurements of Sueoka and co-workers [8,9]. Again we see that agreement between theory and experiment is very good particularly above 20 eV. In general, $\sigma_t(\text{NH}_3) > \sigma_t(\text{H}_2\text{O})$, a situation similar to the electron case [52].

The σ_t values for the isoelectronic molecules CO, N₂, and C₂H₂ are depicted, respectively, in Figs. 5, 6, and 7. For the CO and N₂ cases, our theoretical results are in excellent agreement with all sets of different experimental data at and above 30 eV. However, below 30 eV, our model underestimates experimental values by a significant amount. For the C₂H₂ case, the only measurements are due to Sueoka's group. We need more experimental studies on this molecule in order to see the quality of present results at and above 20 eV. We see that

$$\sigma_t(\text{C}_2\text{H}_2) > \sigma_t(\text{CO}) > \sigma_t(\text{N}_2).$$

The e^+ -O₂ total cross sections are shown in Fig. 8 along with measured values of Refs. [7] and [1]. The weak peaking behavior in the energy dependence of σ_t , as observed in both the experimental data around 60 eV, is faithfully reproduced by our calculations. Our theoretical curve (Fig. 8) is in excellent agreement with both the measurements at and above 20 eV. For heavier gases, such as the SiH₄, CO₂, N₂O, and CF₄, our calculated σ_t are shown in Figs. 9–12. For silane, our results are in very good agreement with the only available experimen-

TABLE II. Molecular parameters (for details see the text).

Molecule	α_0 (a_0^3)	E_{Ps} (eV)	c [Eq. (7)]	a	b
H ₂	5.42	8.62	2.0	956.57	1.1354
CH ₄	17.5	6.18	2.0	827.17	0.9091
NH ₃	15.0	6.20	1.5	563.58	0.8767
H ₂ O	11.0	5.20	1.0	361.55	0.8348
CO	13.16	7.21	1.5	896.36	0.916
N ₂	11.80	8.78	1.75	862.04	0.9134
C ₂ H ₂	22.5	4.61	1.5	1663.54	0.9687
O ₂	10.7	5.27	0.8	1194.27	0.9763
SiH ₄	30.5	4.60	2.0	457.52	0.7631
CO ₂	17.9	6.80	1.0	982.93	0.9093
N ₂ O	20.45	6.09	1.0	1151.61	0.9396
CF ₄	25.9	9.40	1.0	1622.99	0.9591

tal data of Sueoka and Mori [6] (see Fig. 9). For CO₂, our results are in excellent agreement even around 10 eV. At and above 15 eV, our calculated values agree within 5% with all the measured data plotted in Fig. 10. Further, in Figs. 11 and 12, we again find a very good agreement between theory and experiment at energies where experimental data are available.

It is interesting to note that our present model is consistently describing the σ_t quantity in excellent agreement with experiment for all the molecular gases studied in this paper. Although we have shown our calculations from 10 eV, the validity of the present theory is above the ionization threshold or roughly above 20 eV. We could not find a single theoretical calculation in the present energy regime for any of the molecules presented here. From this standpoint, this work will prove to be very useful for existing experimental work and also for future laboratory investigations.

As mentioned earlier, the energy-dependent form of the absorption potential [Eq. (7)] was derived semiempirically in such a way that it works well in the whole energy region (particularly between 20 and 5000 eV) for any target. An *ab initio* determination of V_{abs}^+ is an extremely difficult task and this has not been achieved even for any atomic system. In the past, Joachain and Potvliege [50] have used an electron absorption potential (V_{abs}^-) for the case of positron-Ar scattering. It is therefore worthwhile to derive an approximate form of the positron-molecule effective potential which describes the σ_t parameter quite successfully.

In order to further see the quality of the present absorption potential, which is mainly composed of Ps formation, dissociation, and total ionization cross sections, in Fig. 13, we have shown our positron-H₂ σ_{abs} along with experimental results of Ref. [51]. The measured points in Fig. 13 are a sum of total ionization and Ps formation channels for the positron-H₂ case. We see that our σ_{abs} curve is in fair agreement with observed inelastic cross sections. For other gases too, our σ_{abs} values (not shown) should be very close to the total ionization plus Ps formation cross sections.

Finally, in order to make a simple use of present σ_t data for all the molecules, we have fitted a simple analytic form $\sigma_t(E) = aE^{-b}$ (where E is in eV and σ_t is in units of

10^{-16} cm^2) to our total-cross-section values in the range of 300–5000 eV. This particular form was chosen because it is a generalized formula for charged particles scattered from the polarization potential field in which case $b = \frac{1}{2}$. The values a and b for all the molecules are given in Table II. The above fit is better than 1% (for $E \geq 400$ eV) for molecules such as H₂, H₂O, NH₃, SiH₄, CO₂, N₂O, and CF₄. For other molecules (CH₄, C₂H₂, N₂, O₂, and CO) the present fit is better than 5% for energies at and above 400 eV.

V. CONCLUSIONS

We presented the total (elastic plus inelastic) cross sections of intermediate- and high-energy positron impact with a large variety of molecules, where experimental studies have been carried out recently. We are unaware of previous calculations on any of the present targets. It is well known that in the first-order Born approximation (FBA), the scattering parameters do not depend upon the charge of the projectile. Nevertheless, the FBA theory is not good in the present energy region for both the projectiles. Therefore the present calculations are important where the scattering parameter is derived by employing molecular wave functions. A complex optical potential is derived for each system from target wave functions and its spherical part is employed to yield total cross sections under the complex phase-shift analysis. At and above 30 eV, our results for all the molecules studied here are in very good agreement with available measurements. Below 30 eV, we have discussed the limitations of the present theory. The calculated total cross sections are fitted to a simple formula and the parameters of this analytic expression are provided.

ACKNOWLEDGMENTS

This research is funded by the Research Corporation, Tucson, Arizona under Contract No. C-2924. This work is also partially supported by the U.S. Army Office of Scientific Research under Contract No. DAAL03-89-9-0111. We thank the Florida State University Supercomputer Research Institute (SCRI) for providing supercomputing time.

*Permanent address: Department of Physics and Astrophysics, University of Delhi, Delhi 110007, India.

- [1] M. Charlton, T. C. Griffith, G. R. Heyland, and G. L. Wright, *J. Phys. B* **13**, L353 (1980).
- [2] K. R. Hoffman, M. S. Dababneh, Y.-F. Hsieh, W. E. Kauppila, V. Pol, J. H. Smart, and T. S. Stein, *Phys. Rev. A* **25**, 1393 (1982).
- [3] A. Deuring, K. Floeder, D. Fromme, W. Raith, A. Schwab, G. Sinapius, G. Zitzewitz, and P. W. Krug, *J. Phys. B* **16**, 1633 (1983).
- [4] M. Charlton, T. C. Griffith, G. R. Heyland, and G. L. Wright, *J. Phys. B* **16**, 323 (1983).
- [5] K. Floeder, D. Fromme, W. Raith, A. Schwab, and G. Sinapius, *J. Phys. B* **18**, 3347 (1985).

- [6] O. Sueoka and S. Mori, *J. Phys. B* **19**, 4035 (1986).
- [7] M. S. Dababneh, Y.-F. Hsieh, W. E. Kauppila, Ch. K. Kwan, S. J. Smith, T. S. Stein, and M. N. Uddin, *Phys. Rev. A* **38**, 1207 (1988).
- [8] O. Sueoka, S. Mori, and K. Katayama, *J. Phys. B* **20**, 3237 (1987).
- [9] O. Sueoka, S. Mori, and K. Katayama, *J. Phys. B* **19**, L373 (1986).
- [10] O. Sueoka and S. Mori, *J. Phys. Soc. Jpn.* **53**, 2491 (1984).
- [11] J. Dutton, C. J. Evans, and H. L. Mansour, *J. Phys. B* **20**, 2607 (1987).
- [12] C. J. Evans and H. L. Mansour, *J. Phys. B* **20**, 5925 (1987).
- [13] Ch. K. Kwan, Y.-F. Hsieh, W. E. Kauppila, S. J. Smith, T. S. Stein, M. N. Uddin, and M. S. Dababneh, *Phys. Rev. A*

- 27, 1328 (1983).
- [14] O. Sueoka and S. Mori, *J. Phys. B* **22**, 963 (1989).
- [15] Ch. K. Kwan, Y.-F. Heish, W. E. Kauppila, S. J. Smith, T. S. Stein, M. N. Uddin, and M. S. Dababneh, *Phys. Rev. Lett.* **52**, 1417 (1984).
- [16] O. Sueoka, in *Atomic Physics with Positrons*, edited by J. W. Humberston and E. A. G. Armour (Plenum, New York, 1987), p. 41.
- [17] O. Sueoka, *J. Phys. B* **21**, L631 (1988).
- [18] A. Jain, *Phys. Rev. A* **35**, 4826 (1987).
- [19] A. Jain, in *Positron Annihilation Studies of Fluids*, edited by S. C. Sharma and D. M. Schrader (World Scientific, Singapore, 1987).
- [20] A. Jain, *J. Phys. B* **19**, L807 (1986).
- [21] T. C. Griffith and G. R. Heyland, *Phys. Rep.* **39C**, 169 (1978).
- [22] W. E. Kauppila and T. S. Stein, *Can. J. Phys.* **60**, 471 (1982).
- [23] M. Charlton, *Rep. Prog. Phys.* **48**, 737 (1985).
- [24] T. C. Griffith, *Adv. At. Mol. Phys.* **22**, 37 (1986).
- [25] T. S. Stein and W. E. Kauppila, *Adv. At. Mol. Phys.* **18**, 53 (1982).
- [26] T. S. Stein and W. E. Kauppila, in *Electronic and Atomic Collisions*, edited by D. C. Lorentz *et al.* (Elsevier, New York, 1986), p. 105.
- [27] C. Szmytkowski, *Z. Phys. D* **13**, 69 (1989).
- [28] E. A. G. Armour, *Phys. Rep.* **169**, 198 (1988).
- [29] A. Jain, *J. Chem. Phys.* **78**, 6579 (1983); *Phys. Rev. A* **34**, 3707 (1986).
- [30] A. Jain and K. L. Baluja, *Phys. Rev. A* **45**, 202 (1992).
- [31] For example, see N. F. Lane, *Rev. Mod. Phys.* **41**, 92 (1980), and references therein.
- [32] F. A. Gianturco and A. Jain, *Phys. Rep.* **143**, 347 (1986).
- [33] A. Jain, *Phys. Rev. A* **41**, 2437 (1990).
- [34] A. Jain, *J. Phys. B* **23**, 863 (1991).
- [35] A. Jain (unpublished).
- [36] J. K. O'Connell and N. F. Lane, *Phys. Rev. A* **27**, 1893 (1983).
- [37] N. T. Padial and D. W. Norcross, *Phys. Rev. A* **29**, 1742 (1984).
- [38] F. A. Gianturco, A. Jain, and L. C. Pantano, *J. Phys. B* **20**, 571 (1987).
- [39] A. Jain and F. A. Gianturco, *J. Phys. B* **24**, 2387 (1991).
- [40] T. Mukherjee, A. S. Ghosh, and A. Jain, *Phys. Rev. A* **43**, 2358 (1991).
- [41] A. Jain, in *Positrons and Positronium Chemistry*, edited by Y. C. Jean (World Scientific, Singapore, 1991), p. 199.
- [42] M. A. Morrison, *Comput. Phys. Commun.* **21**, 63 (1980).
- [43] F. A. Gianturco, D. G. Thompson, and A. Jain (private communication).
- [44] K. L. Baluja and A. Jain (unpublished).
- [45] A. D. McLean and M. Yoshmine, *Int. J. Quantum Chem.* **1S**, 313 (1967).
- [46] P. E. Cade and A. C. Wahl, *At. Data Nucl. Data Tables* **13**, 339 (1974).
- [47] F. A. Gianturco (private communication).
- [48] G. Staszewska, D. W. Schwenke, D. Thirumalai, and D. G. Truhlar, *J. Phys. B* **16**, L281 (1983); *Phys. Rev. A* **28**, 2740 (1983); G. Staszewska, D. W. Schwenka, and D. G. Truhlar, *J. Chem. Phys.* **81**, 335 (1984); *Phys. Rev. A* **29**, 3078 (1984).
- [49] F. Calogero, *Variable Phase Approach to Potential Scattering* (Academic, New York, 1974).
- [50] C. J. Joachain and R. M. Potvliege, *Phys. Rev. A* **35**, 4873 (1987).
- [51] D. Fromme, G. Kruse, W. Raith, and G. Sinapius, *J. Phys. B* **21**, L261 (1988).
- [52] A. Jain, *J. Phys. B* **22**, 905 (1988).